

Low-lying electronic states of osmium monoxide OsO

Wen Yan(严汶) and Wenli Zou(邹文利)
Citation: Chin. Phys. B, 2023, 32 (**11**): 113101. DOI: 10.1088/1674-1056/acec46
Journal homepage: http://cpb.iphy.ac.cn; http://iopscience.iop.org/cpb

What follows is a list of articles you may be interested in

Molecule opacity study on low-lying states of CS

Rui Li(李瑞), Jiqun Sang(桑纪群), Xiaohe Lin(林晓贺), Jianjun Li(李建军), Guiying Liang(梁桂颖), and Yong Wu(吴勇)
Chin. Phys. B, 2022, 31 (**10**): 103101. DOI: 10.1088/1674-1056/ac834f

Relativistic calculations on the transition electric dipole moments and radiative lifetimes of the spin-forbidden transitions in the antimony hydride molecule

Yong Liu(刘勇), Lu-Lu Li(李露露), Li-Dan Xiao(肖利丹), and Bing Yan(闫冰)
Chin. Phys. B, 2022, 31 (**8**): 083101. DOI: 10.1088/1674-1056/ac6ee1

Theoretical study on the transition properties of AlF

Yun-Guang Zhang(张云光), Ling-Ling Ji(吉玲玲), Ru Cai(蔡茹),Cong-Ying Zhang(张聪颖), and Jian-Gang Xu(徐建刚)
Chin. Phys. B, 2022, 31 (**5**): 053101. DOI: 10.1088/1674-1056/ac3648

Configuration interaction study on low-lying states of AlCl molecule

Xiao-Ying Ren(任笑影), Zhi-Yu Xiao(肖志宇), Yong Liu(刘勇), and Bing Yan(闫冰)
Chin. Phys. B, 2021, 30 (**5**): 053101. DOI: 10.1088/1674-1056/abd46a

Vibronic spectra of aluminium monochloride relevant to circumstellar molecule

Jian-Gang Xu(徐建刚), Cong-Ying Zhang(张聪颖), Yun-Guang Zhang(张云光)
Chin. Phys. B, 2020, 29 (**3**): 033102. DOI: 10.1088/1674-1056/ab6c46

SPECIAL TOPIC — Celebrating the 100th Anniversary of Physics Discipline of Northwest University

Low-lying electronic states of osmium monoxide OsO

Wen Yan(严汶)[1,2] and Wenli Zou(邹文利)[1,2,†]

[1] *Institute of Modern Physics, Northwest University, Xi'an* 710127, *China*
[2] *Shaanxi Key Laboratory for Theoretical Physics Frontiers, Xi'an* 710127, *China*

(Received 22 June 2023; revised manuscript received 21 July 2023; accepted manuscript online 1 August 2023)

The ground state of osmium monoxide (OsO) has long been controversial. In this paper, the low-lying Λ–S and Ω electronic states of OsO have been comprehensively studied by the high-precision multi-reference calculations. The ground state of OsO is unexpectedly the closed-shell $^1\Sigma^+$ state with a double bond instead of the previously reported $^3\Phi$ or $^5\Sigma^+$ state; after including the spin–orbit coupling effects, the ground state becomes $^3\Pi_2$. With the help of the theoretical spectroscopic constants and transition dipole moments, the emission spectra in the region of 405 nm–875 nm are assigned. Our results will facilitate the future studies of absorption and emission spectra of OsO.

Keywords: transition dipole moment, multi-reference second-order perturbation theory, spin–orbit coupling, exact two-component

PACS: 31.15.A–, 31.15.aj, 31.15.am, 36.20.Kd **DOI:** 10.1088/1674-1056/acec46

1. Introduction

Transition metal-containing small molecules are known to pose challenges to spectral assignments. In addition to the strong spin–orbit coupling (SOC) effects, the abundance electronic configurations, the dense distribution of electronic states, and the high angular quantum numbers make the assignment of electronic spectra rather complicated. In this respect, the high-precision theoretical calculations by multi-reference methods play crucial roles in assisting experimental assignments. However, the multi-reference methods are not black-box tools, which hinders their widespread applications. In a recent paper[1] we studied the low-lying electronic states of the osmium monoxide cation (OsO^+), and in the present work, we focus on the neutral OsO molecule because its emission spectra measured nearly 40 years ago[2] have not been assigned until now.

Both experimental and theoretical studies of OsO are scarce. Gatterer *et al.*[3] and Raziunas *et al.*[4] reported the earliest emission spectra of OsO in 1957 and in 1965, respectively, but no analyses were made. Weltner suggested a possible ground state $^5\Sigma$ in a review published in 1978.[5] In 1984, Balfour and Ram[2] photographed the emission spectra of OsO in the region 405 nm–875 nm, in which many bands had been observed. However, they could not determine the spectral term of the ground state. The candidate ground states of OsO were theoretically studied only at the density functional theory (DFT) level of theory without considering the SOC effects, which could be either $^3\Phi$ or $^5\Sigma^+$ depending on the functionals.[6–8] Due to the fact that the first-order SOC constant of $^5\Sigma^+$ is zero, one may speculate that the ground Ω state of OsO comes probably from $^3\Phi$. However, this is not true according to our results in this study. On the whole, the ground state and the assignments of the experimental emission bands of OsO are still not known.

This paper is structured as follows. Some computational details are given first. In the subsequent section, the low-lying Λ–S and Ω states of OsO have been studied by high-precision multi-reference calculations, which are used to assign the emission bands. Important findings of this work are summarized in the Conclusion section.

2. Theoretical method

The scalar relativistic effects are taken into account via the exact two-component (X2C) Hamiltonian,[9,10] which is combined with the relativistically contracted 4-ζ quality ANO-R3 basis set[11,12] and the finite size nuclear model. Totally 43 low-lying Λ–S states of OsO below 3×10^4 cm^{-1} are calculated using SA-CASSCF (state-averaged complete active space self-consistent field) with the C_{2v} point group symmetry, including fourteen singlet, twenty triplet, eight quintet, and one septet ones (see Table 1). Based on the SA-CASSCF wavefunctions, two multi-reference methods have been used in this study to take dynamic correlations into account, i.e., RMS-CASPT2 (rotated multi-state complete active space second-order perturbation theory)[13] and MS-NEVPT2 (multi-state partially contracted *n*-electron valence state second order perturbation theory).[14] The active space consists of 12 electrons in 9 molecular orbitals (MOs), i.e. CAS(12e,9o), corresponding to the 5d6s shells of Os and the 2p shell of O. All the occupied MOs below the active space are relaxed in the

†Corresponding author. E-mail: zouwl@nwu.edu.cn

© 2023 Chinese Physical Society and IOP Publishing Ltd

SA-CASSCF calculations, whereas in the RMS-CASPT2 and MS-NEVPT2 calculations the 24 electrons in the MOs corresponding to O 2s and semi-core shells Os 4f5s5p are also correlated. The resulted total number of configurations for singlet, triplet, and quintet states are approximately 9×10^9, 18×10^9, and 3×10^9, respectively. Since CASPT2 suffers from the intruder state problem, an imaginary level shift[15] of 0.25 a.u. (atomic unit) and an IPEA level shift[16] of 0.25 a.u. are used together, which lead to the weights of the reference states being about 81%.

The SOC effects are considered via the biorthonormal state-interaction (SI) approach[17] with the one-center atomic mean field integral (AMFI) approximation[18] for one- and two-electron spin–orbit integrals. The perturbatively modified CASSCF (PM-CASSCF) wavefunctions by RMS-CASPT2 are adopted to construct the spin–orbit matrix, where the diagonal elements are replaced by the corresponding RMS-CASPT2 or MS-NEVPT2 energies calculated above. More technical details about SOC calculations may be found in Ref. [19].

The BDF quantum chemistry program package[20] is used for the quadratically convergent SA-CASSCF calculations, whereas the MS-NEVPT2 calculations are carried out using the Xi'an-CI program package[21] that interfaces with BDF. The transformed SA-CASSCF wavefunctions are also passed to the OpenMolcas program package[22,23] to perform the RMS-CASPT2 and subsequent SI calculations. Since the double group symmetry is not implemented in the SI approach of OpenMolcas, the in-house Fortran90 program OmSym-II is used to identify the Ω states. Based on the potential energy curves (PECs) of Λ–S or Ω states, the spectroscopic constants are fitted by numerically solving the one-dimensional Schrödinger equation using Le Roy's LEVEL program,[24] including the adiabatic excitation energy (T_e), the equilibrium bond length (R_e), the vibrational frequency (ω_e), and the rotational constant (B_e).

3. Results and discussion

3.1. Λ–S states of OsO

The PECs of the Λ–S states by MS-NEVPT2 are plotted in Fig. 1. The fitted spectroscopic constants are collected in Table 1, and are compared with the ones by RMS-CASPT2.

Both the RMS-CASPT2 and MS-NEVPT2 results show that the ground Λ–S state of OsO is the closed-shell $[1]^1\Sigma^+$ whereas the first excited state $[1]^3\Pi$ is only one or two hundred wavenumbers higher in energy, thus the other candidate ground states $[1]^3\Phi$ and $[1]^5\Sigma^+$ in early DFT studies[6–8] are completely denied. The excitation energies of the higher Λ–S states by RMS-CASPT2 and MS-NEVPT2 are basically coincident, but the energy differences can be 0.2 eV (about 1600 cm^{-1}) or even larger in some states, for example, $[1]^3\Phi$ and $[1]^5\Sigma^+$. To verify those inconsistent results, the more accurate SDSCI+P (static-dynamic-static multi-reference configuration interaction with Pople's cluster corrections)[25,26] calculations are performed at the bond distance of 1.66 Å with the same active space and frozen core electrons, and the results compare well with the MS-NEVPT2 ones with the maximum error of about 500 cm^{-1}. By comparisons, the RMS-CASPT2 underestimates the energies of $[1]^3\Phi$ and $[1]^5\Sigma^+$ by about 800 cm^{-1} and 2200 cm^{-1}, respectively. Consequently, only the MS-NEVPT2/SI results are reported in the following subsection.

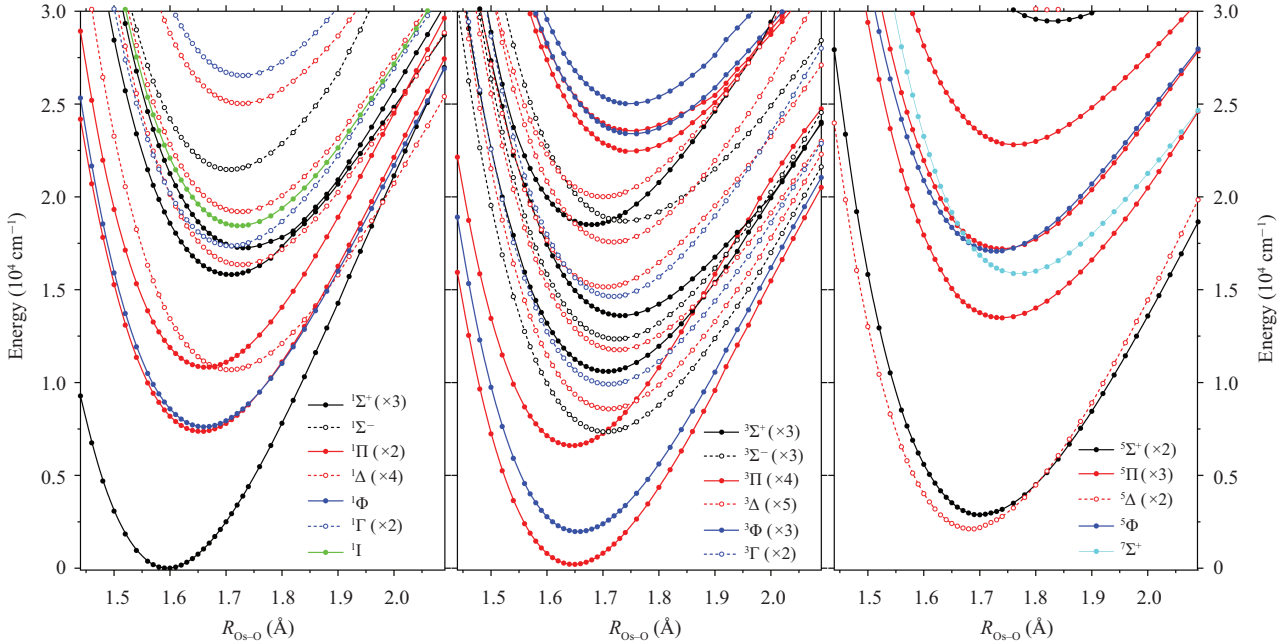


Fig. 1. The PECs of low-lying Λ–S states of OsO by MS-NEVPT2.

Table 1. Spectroscopic constants of Λ–S states of $^{192}Os^{16}O$ by RMS-CASPT2 and MS-NEVPT2.

Λ–S state	Method[a]	T_e (cm^{-1})	R_e (Å)	ω_e (cm^{-1})	B_e (cm^{-1})	Dominant configurations[b] $1\sigma/2\sigma/3\sigma/1\pi/2\pi/1\delta$ ($\geq 10\%$)
$[1]^1\Sigma^+$	(A)	0	1.603	1116	0.4402	220404 (82)
	(B)	0	1.595	1135	0.4464	
$[2]^1\Sigma^+$	(A)	15069	1.728	961	0.3805	220422 (69) + 210423 (20)
	(B)	15811	1.708	951	0.3908	
$[3]^1\Sigma^+$	(A)	19649	1.724	923	0.3820	210423 (40) + 200424 (31) + 220422 (18)
	(B)	17253	1.733	880	0.3740	
$[1]^1\Sigma^-$	(A)	22909	1.715	938	0.3860	210423 (90)
	(B)	21467	1.707	943	0.3896	
$[1]^1\Pi$	(A)	9066	1.669	1009	0.4074	220413 (83)
	(B)	7368	1.656	1036	0.4143	
$[2]^1\Pi$	(A)	10982	1.664	1030	0.4102	210414 (86)
	(B)	10820	1.664	1022	0.4099	
$[1]^1\Delta$	(A)	12604	1.720	954	0.3852	210423 (55) + 220422 (23) + 200424 (14)
	(B)	10683	1.707	946	0.3896	
$[2]^1\Delta$	(A)	16634	1.723	893	0.3802	220422 (68) + 210423 (10) + 200424 (10)
	(B)	16342	1.728	920	0.3802	
$[3]^1\Delta$	(A)	20033	1.734	896	0.3748	210423 (51) + 220422 (30)
	(B)	19201	1.726	897	0.3833	
$[4]^1\Delta$	(A)	26372	1.722	892	0.3835	210423 (44) + 220422 (32) + 200424 (12)
	(B)	25019	1.729	896	0.3819	
$[1]^1\Phi$	(A)	5658	1.667	1066	0.4104	220413 (87)
	(B)	7610	1.661	1031	0.4116	
$[1]^1\Gamma$	(A)	17748	1.715	979	0.3848	210423 (58) + 220422 (33)
	(B)	17357	1.710	935	0.3884	
$[2]^1\Gamma$	(A)	26090	1.730	878	0.3813	220422 (55) + 210423 (33)
	(B)	26534	1.730	904	0.3811	
$[1]^1I$	(A)	16478	1.727	926	0.3807	220422 (91)
	(B)	18440	1.723	928	0.3821	
$[1]^3\Sigma^+$	(A)	10851	1.719	940	0.3834	220422 (65) + 210423 (16)
	(B)	10597	1.706	919	0.3899	
$[2]^3\Sigma^+$	(A)	13750	1.748	831	0.3777	210423 (57) + 220422 (14) + 211404 (12)
	(B)	13600	1.734	861	0.3772	
$[3]^3\Sigma^+$	(A)	17747	1.711	1101	0.3941	211404 (70) + 210423 (12)
	(B)	18503	1.680	943	0.4063	
$[1]^3\Sigma^-$	(A)	8065	1.721	908	0.3830	220422 (43) + 210423 (30) + 200424 (13)
	(B)	7346	1.705	950	0.3906	
$[2]^3\Sigma^-$	(A)	13339	1.731	886	0.3796	220422 (45) + 210423 (22) + 200424 (15)
	(B)	12343	1.725	882	0.3818	
$[3]^3\Sigma^-$	(A)	18081	1.739	867	0.3751	220422 (46) + 210423 (33)
	(B)	18692	1.739	838	0.3746	
$[1]^3\Pi$	(A)	101	1.657	1042	0.4135	220413 (76)
	(B)	204	1.647	1045	0.4184	
$[2]^3\Pi$	(A)	7989	1.661	1008	0.4113	210414 (65)
	(B)	6597	1.644	1061	0.4194	
$[3]^3\Pi$	(A)	22030	1.761	834	0.3657	211413 (42) + 221412 (35)
	(B)	22450	1.745	840	0.3697	
$[4]^3\Pi$	(A)	23549	1.756	815	0.3674	211413 (63) + 201414 (10)
	(B)	23537	1.755	837	0.3685	
$[1]^3\Delta$	(A)	8960	1.715	961	0.3831	220422 (47) + 210423 (35)
	(B)	8576	1.711	949	0.3879	
$[2]^3\Delta$	(A)	12176	1.725	840	0.3791	210423 (62) + 220422 (19)
	(B)	11761	1.726	874	0.3806	
$[3]^3\Delta$	(A)	16075	1.712	931	0.3855	210423 (75)
	(B)	15145	1.704	918	0.3899	
$[4]^3\Delta$	(A)	17575	1.709	1023	0.3900	221403 (75)
	(B)	17563	1.719	938	0.3843	
$[5]^3\Delta$	(A)	18913	1.723	901	0.3826	210423 (76)
	(B)	20004	1.702	902	0.3919	
$[1]^3\Phi$	(A)	554	1.659	1018	0.4109	220413 (83)
	(B)	1967	1.655	1038	0.4142	
$[2]^3\Phi$	(A)	23601	1.749	826	0.3682	211413 (79)
	(B)	23387	1.752	839	0.3692	

(Continued on the next page)

$[3]^3\Phi$	(A)	24831	1.754	820	0.3689	211413 (82)
	(B)	25008	1.748	846	0.3739	
$[1]^3\Gamma$	(A)	10913	1.710	927	0.3841	210423 (61) + 220422 (26)
	(B)	9908	1.710	916	0.3877	
$[2]^3\Gamma$	(A)	13772	1.723	964	0.3817	220422 (59) + 210423 (25)
	(B)	14633	1.719	926	0.3842	
$[1]^5\Sigma^+$	(A)	228	1.716	948	0.3863	220422 (87)
	(B)	2869	1.697	997	0.3906	
$[2]^5\Sigma^+$	(A)	27644	1.839	705	0.3353	211422 (78) + 211332 (14)
	(B)	29463	1.830	696	0.3380	
$[1]^5\Pi$	(A)	13182	1.752	853	0.3696	211413 (44) + 210432 (21) + 221412 (20)
	(B)	13482	1.740	866	0.3751	
$[2]^5\Pi$	(A)	17033	1.765	741	0.3685	210432 (58) + 211413 (11) + 221412 (10)
	(B)	17203	1.737	845	0.3765	
$[3]^5\Pi$	(A)	19571	1.760	767	0.3664	221412 (47) + 211413 (28)
	(B)	22803	1.760	803	0.3674	
$[1]^5\Delta$	(A)	2949	1.709	1023	0.3908	210423 (86)
	(B)	2107	1.686	1066	0.3995	
$[2]^5\Delta$	(A)	28043	1.834	661	0.3349	211422 (76) + 211332 (10)
	(B)	30072	1.824	665	0.3403	
$[1]^5\Phi$	(A)	15875	1.745	881	0.3719	211413 (84)
	(B)	17070	1.729	902	0.3795	
$[1]^7\Sigma^+$	(A)	13935	1.788	809	0.3553	211422 (93)
	(B)	15854	1.770	889	0.3614	

[a] (A) RMS-CASPT2; (B) MS-NEVPT2.
[b] 1σ: O $2p_\sigma$, 2σ: Os $5d_\sigma 6s$, 3σ: Os $5d_\sigma 6s$ + O $2p_\sigma$, 1π: O $2p_\pi$ + Os $5d_\pi$, 2π: Os $5d_\pi$ + O $2p_\pi$, 1δ: Os $5d_\delta$.

Using the SA-CASSCF wavefunctions, the Wiberg bond indices (WBIs) in the NAO (natural atomic orbital) basis[27] are calculated for the lowest five Λ–S states below 3000 cm^{-1}. It is found that the OsO molecule has a double bond in $[1]^1\Sigma^+$ (WBI = 1.9), a one and a half bond in $[1]^3\Pi$ and $[1]^3\Phi$ (WBI = 1.5), and a single bond in $[1]^5\Sigma^+$ and $[1]^5\Delta$ (WBI = 1.2). The bond strength n is also reflected in the equilibrium bond length through an approximate Badger relationship $n = |a|r_e^{-|b|}$ (although there are some counter examples in the literatures[28,29]). Among the lowest five Λ-S states, the bond orders may be confirmed further by the qualitatively consistent bond lengths: $[1]^1\Sigma^+$ has the shortest bond length of about 1.60 Å, $[1]^3\Pi$ and $[1]^3\Phi$ present the medium bond length of about 1.66 Å, whereas the longest bond length of about 1.70 Å exists in the two quintet states $[1]^5\Sigma^+$ and $[1]^5\Delta$.

3.2. Ω states of OsO

At the MS-NEVPT2/SI level of theory, the PECs of the low-lying Ω states below 2.5×10^4 cm^{-1} are shown in Fig. 2, and the spectroscopic constants are summarized in Table 2. The Ω states higher than 2.5×10^4 cm^{-1} are expected to be unreliable due to insufficient auxiliary Λ–S states in the spin–orbit matrix and therefore are not reported.

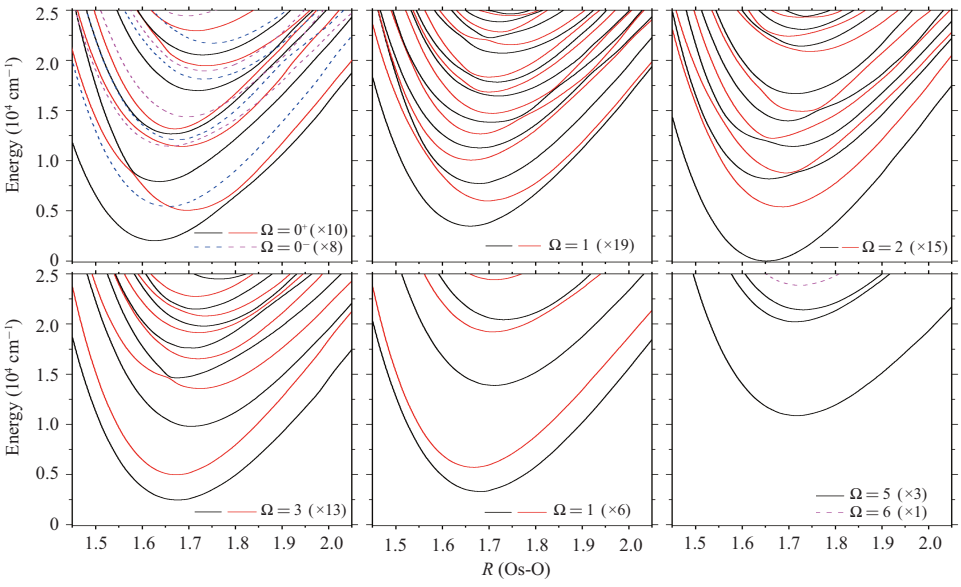


Fig. 2. The PECs of low-lying Ω states of OsO by MS-NEVPT2/SI.

After including SOC, the lowest five Λ–S states aforementioned lead to the fifteen Ω states below 9×10^3 cm^{-1} (i.e. $\{1-3\}0^+$, $\{1\}0^-$, $\{1-3\}1$, $\{1-4\}2$, $\{1-2\}3$, and $\{1-2\}4$) as well as two additional Ω states $\{2-3\}0^-$. Since the ground Λ–S state $[1]^1\Sigma^+$ does not split, the $\Omega=2$ branch of the first excited Λ–S state $[1]^3\Pi$ becomes the ground Ω state. Accordingly the bond order of OsO in its ground state decreases from a double bond to a one and a half bond. In addition to $\{1\}2$, the $[1]^3\Pi$ state also splits into the first $\Omega=0^+$, 0^-, and 1 sub-states, but in the former two sub-states some of the other Λ–S states also make significant contributions.

Table 2. Spectroscopic constants of Ω states of ^{192}Os^{16}O by MS-NEVPT2/SI.

Ω state	T_e (cm^{-1})	R_e (Å)	ω_e (cm^{-1})	B_e (cm^{-1})	$\lvert\mu\rvert^2$ (a.u.)					Dominant Λ–S states (≥ 10%)
					{1}2	{1}0^+	{1}3	{1}4	{1}1	
{1}0^+	2035	1.627	992	0.4291						$[1]^1\Sigma^+$ (50) + $[1]^3\Pi$ (38)
{2}0^+	5021	1.698	1083	0.3927		0.003				$[1]^5\Sigma^+$ (67) + $[1]^3\Sigma^-$ (19)
{3}0^+	7921	1.637	1081	0.4216		0.001				$[1]^1\Sigma^+$ (38) + $[1]^5\Delta$ (33) + $[2]^3\Pi$ (22)
{4}0^+	11426	1.685	925	0.4023					0.017	$[1]^3\Sigma^-$ (46) + $[1]^5\Sigma^+$ (17) + $[2]^1\Sigma^+$ (13)
{5}0^+	12673	1.665	1012	0.4099		0.001				$[2]^3\Pi$ (61) + $[1]^5\Delta$ (31)
{6}0^+	13170	1.670	1199	0.4063		0.016			0.034	$[1]^3\Pi$ (36) + $[1]^3\Sigma^-$ (17) + $[2]^1\Sigma^+$ (12)
{7}0^+	16987	1.719	922	0.3838					0.099	$[2]^3\Sigma^-$ (43) + $[1]^5\Pi$ (18) + $[2]^1\Sigma^+$ (16)
{8}0^+	19464	1.738	853	0.3745		0.004			0.004	$[1]^5\Pi$ (67) + $[3]^1\Sigma^+$ (11)
{9}0^+	20540	1.731	866	0.3817		0.001			0.007	$[3]^3\Sigma^-$ (38) + $[2]^3\Sigma^-$ (34) + $[3]^1\Sigma^+$ (18)
{10}0^+	22950	1.716	902	0.3875		0.001			0.002	$[2]^1\Sigma^+$ (51) + $[3]^1\Sigma^+$ (26)
{1}0^-	5432	1.656	1017	0.4148						$[1]^3\Pi$ (45) + $[2]^3\Pi$ (26) + $[1]^5\Delta$ (24)
{2}0^-	11447	1.659	962	0.4113					0.006	$[1]^3\Pi$ (50) + $[2]^3\Pi$ (33)
{3}0^-	12086	1.676	1044	0.4052					0.002	$[1]^5\Delta$ (68) + $[2]^3\Pi$ (20)
{4}0^-	14367	1.695	1041	0.3947					0.010	$[1]^3\Sigma^+$ (51) + $[2]^3\Pi$ (23) + $[1]^5\Pi$ (15)
{5}0^-	18128	1.734	897	0.3767					0.034	$[2]^3\Sigma^+$ (43) + $[1]^5\Pi$ (24) + $[1]^3\Sigma^+$ (21)
{6}0^-	18956	1.736	878	0.3775					0.020	$[2]^3\Sigma^+$ (43) + $[1]^5\Pi$ (25) + $[1]^7\Sigma^+$ (14)
{7}0^-	21697	1.751	902	0.3704					0.002	$[1]^7\Sigma^+$ (60) + $[2]^5\Pi$ (18) + $[1]^5\Pi$ (15)
{8}0^-	24418	1.699	904	0.3920					0.008	$[3]^3\Sigma^+$ (65) + $[3]^5\Pi$ (15)
{1}1	3485	1.660	1003	0.4124						$[1]^3\Pi$ (74) +$[1]^5\Delta$ (11)
{2}1	5971	1.698	1074	0.3925	0.004				0.012	$[1]^5\Sigma^+$ (65) + $[1]^3\Sigma^-$ (22)
{3}1	7723	1.679	1026	0.4031	0.007	0.005			0.033	$[1]^5\Delta$ (63) + $[1]^3\Pi$ (10)
{4}1	10055	1.662	1006	0.4102	0.002	0.024				$[2]^3\Pi$ (54) + $[1]^5\Delta$ (12) + $[1]^3\Sigma^+$ (10)
{5}1	11276	1.679	926	0.4032	0.028	0.047			0.009	$[1]^1\Pi$ (33) + $[1]^3\Sigma^-$ (15) + $[1]^3\Pi$ (15)
{6}1	12676	1.681	1069	0.4028	0.068	0.004			0.020	$[1]^1\Pi$ (47) + $[1]^3\Sigma^-$ (22)
{7}1	13830	1.708	830	0.3941	0.028	0.050				$[1]^3\Sigma^+$ (21) + $[2]^3\Sigma^-$ (15) + $[2]^3\Pi$ (14)
{8}1	14713	1.708	964	0.3874	0.065	0.010				$[1]^3\Delta$ (34) + $[2]^1\Pi$ (19) + $[2]^3\Sigma^-$ (16)
{9}1	16449	1.719	866	0.3844	0.024	0.001			0.002	$[1]^5\Pi$ (33) + $[1]^3\Delta$ (19) + $[2]^3\Sigma^+$ (10)
{10}1	16844	1.702	1043	0.3874	0.009	0.011			0.012	$[2]^1\Pi$ (30) + $[1]^5\Pi$ (24)+ $[2]^3\Delta$ (17)
{11}1	17832	1.717	947	0.3857	0.009	0.006			0.011	$[2]^3\Delta$ (35) + $[1]^5\Pi$ (24) + $[2]^3\Sigma^+$ (15)
{12}1	18336	1.703	1007	0.3882	0.014	0.001			0.005	$[2]^3\Delta$ (21) + $[2]^1\Pi$ (17)+ $[1]^3\Delta$ (16)
{13}1	20722	1.728	825	0.3774	0.002	0.005			0.001	$[1]^5\Pi$ (49) + $[1]^3\Sigma^+$ (14) + $[1]^7\Sigma^+$ (12)
{14}1	21544	1.748	902	0.3829		0.001			0.001	$[1]^7\Sigma^+$ (55) + $[2]^5\Pi$ (22) + $[1]^5\Pi$ (14)
{15}1	22241	1.703	908	0.3847	0.001	0.001			0.001	$[3]^3\Delta$ (56) + $[1]^7\Sigma^+$ (13)
{16}1	22828	1.725	980	0.3851		0.018			0.005	$[3]^3\Delta$ (28) + $[2]^3\Sigma^+$ (25) + $[2]^3\Sigma^-$ (24)
{17}1	23845	1.722	900	0.3849		0.003			0.001	$[1]^5\Phi$ (58) + $[4]^3\Delta$ (14)
{18}1	24455	1.749	847	0.3829	0.002	0.002				$[3]^3\Sigma^-$ (42) + $[2]^5\Pi$ (29)
{19}1	24612	1.747	916	0.3813		0.001			0.001	$[2]^5\Pi$ (49) + $[3]^3\Sigma^-$ (16)
{1}2	0	1.653	1027	0.4159						$[1]^3\Pi$ (83)
{2}2	5404	1.685	1051	0.3999	0.012				0.014	$[1]^5\Delta$ (74)
{3}2	8185	1.658	1013	0.4067						$[1]^3\Phi$ (88)
{4}2	8763	1.697	1237	0.3999	0.001					$[1]^5\Sigma^+$ (82)
{5}2	11419	1.710	911	0.3970	0.017		0.013		0.052	$[1]^3\Delta$ (49) + $[1]^1\Delta$ (23)
{6}2	12235	1.665	1281	0.3983	0.007		0.032		0.039	$[2]^3\Pi$ (57) + $[1]^1\Delta$ (13) + $[3]^3\Delta$ (10)
{7}2	13970	1.698	1094	0.3941	0.006		0.136		0.013	$[2]^3\Delta$ (29) + $[2]^3\Pi$ (24) + $[1]^1\Delta$ (20)
{8}2	14921	1.728	977	0.3850	0.014		0.081		0.002	$[1]^5\Pi$ (65)

(Continued on the next page)

{9}2	16683	1.714	926	0.3856	0.012	0.002		0.160	$[2]^3\Delta$ (27) + $[1]^3\Delta$ (25) + $[1]^1\Delta$ (23)
{10}2	20879	1.748	842	0.3744		0.032		0.021	$[1]^7\Sigma^+$ (45) + $[2]^5\Pi$ (25) + $[4]^3\Delta$ (12)
{11}2	21417	1.727	985	0.3791	0.007	0.005		0.007	$[1]^5\Phi$ (46) + $[4]^3\Delta$ (11) + $[1]^7\Sigma^+$ (10)
{12}2	22412	1.704	923	0.3844	0.001	0.017			$[3]^3\Delta$ (59) + $[1]^1\Delta$ (17)
{13}2	23087	1.730	898	0.3817	0.012	0.008		0.002	$[2]^1\Delta$ (47) + $[3]^1\Delta$ (10)
{14}2	24299	1.722	823	0.3835	0.002	0.009		0.046	$[2]^5\Pi$ (49) + $[1]^7\Sigma^+$ (15) + $[4]^3\Delta$ (11)
{15}2	24365	1.740	915	0.3783				0.013	$[4]^3\Delta$ (40) + $[5]^3\Delta$ (12) + $[1]^5\Phi$ (12)
{1}3	2459	1.676	969	0.4048	0.009				$[1]^3\Phi$ (41) + $[1]^5\Delta$ (23) + $[1]^1\Phi$ (15)
{2}3	4972	1.674	1067	0.4056	0.015	0.081			$[1]^5\Delta$ (58) + $[1]^3\Phi$ (24)
{3}3	9802	1.705	951	0.3885	0.167	0.001	0.037		$[1]^3\Delta$ (52) + $[1]^5\Pi$ (17) + $[1]^5\Delta$ (14)
{4}3	13566	1.723	900	0.3805	0.111	0.035	0.010		$[1]^5\Pi$ (56) + $[1]^3\Delta$ (18) + $[2]^3\Delta$ (12)
{5}3	14635	1.666	1223	0.3924	0.068	0.005	0.006		$[1]^1\Phi$ (57) + $[1]^3\Phi$ (20)
{6}3	16531	1.721	920	0.3837	0.011	0.002	0.148		$[2]^3\Delta$ (59) + $[1]^1\Phi$ (16)
{7}3	17606	1.711	976	0.3919		0.004	0.004		$[1]^3\Gamma$ (77)
{8}3	19139	1.724	870	0.3834	0.023	0.006	0.027		$[3]^3\Delta$ (65) + $[4]^3\Delta$ (11)
{9}3	19793	1.733	881	0.3782	0.024	0.001	0.020		$[4]^3\Delta$ (26) + $[1]^5\Phi$ (22) + $[1]^7\Sigma^+$ (18)
{10}3	20791	1.737	897	0.3776	0.002		0.003		$[1]^5\Phi$ (29) + $[1]^7\Sigma^+$ (28) + $[2]^5\Pi$ (20)
{11}3	21501	1.719	992	0.3842			0.008		$[2]^3\Gamma$ (54) + $[2]^5\Pi$ (10) + $[1]^7\Sigma^+$ (10)
{12}3	22746	1.718	939	0.3900	0.007	0.002			$[4]^3\Delta$ (36) + $[1]^5\Phi$ (29) + $[2]^3\Gamma$ (17)
{13}3	24464	1.764	742	0.3682	0.016		0.001		$[2]^5\Pi$ (54) + $[1]^7\Sigma^+$ (36)
{1}4	3298	1.680	1024	0.4025					$[1]^5\Delta$ (72) + $[1]^3\Phi$ (26)
{2}4	5709	1.667	1037	0.4084			0.076		$[1]^3\Phi$ (62) + $[1]^5\Delta$ (33)
{3}4	13873	1.713	958	0.3879		0.098	0.006		$[1]^3\Gamma$ (86)
{4}4	19214	1.706	939	0.3879		0.050			$[2]^3\Gamma$ (70) + $[1]^1\Gamma$ (20)
{5}4	20424	1.732	896	0.3803		0.005			$[1]^5\Phi$ (68) + $[2]^3\Phi$ (19)
{6}4	24416	1.710	913	0.3895		0.003	0.001		$[1]^1\Gamma$ (69) + $[2]^3\Gamma$ (23)
{1}5	10860	1.717	940	0.3848			0.078		$[1]^3\Gamma$ (91)
{2}5	20230	1.714	898	0.3853			0.033		$[2]^3\Gamma$ (84) + $[1]^5\Phi$ (12)
{3}5	21408	1.732	886	0.3804			0.019		$[1]^5\Phi$ (75) + $[2]^3\Gamma$ (21)
{1}6	23848	1.723	926	0.3842					$[1]^1$I (100)

The dominant components of the higher Ω states are more complicated duo to strong SOC effects, and there is not a dominant Λ–S component with the weight lager than 70% except for {7}3 and $\Omega = 4, 5$, and 6 states. Considering the lack of reliable experimental spectroscopic constants for comparison, we will discuss them below combined with the assignment of the experimental emission bands. However, due to the high density of Ω states distributed in the energy range of 1.5×10^4 cm^{-1}–2.5×10^4 cm^{-1}, it is a tough work to identify the experimental emission bands as the calculated upper and lower Ω states. Transition probability is a necessary indicator to distinguish the allowed transitions by selection rule. At 1.66 Å, the squares of total transition dipole moments ($|\mu|^2$) between the lowest five ({1}2, {1}3, {1}0^+, {1}4, and {1}1) and the higher excited Ω states are listed in Table 2, which are proportional to the absorption intensity via the relationship $I_{\rm abs} \propto N''\Delta_{\rm e}|\mu|^2$ with N'' being the population on the lower Ω state due to Boltzmann distribution[30] and $\Delta_{\rm e}$ being the energy difference between two Ω states. Similarly the emission intensity is $I_{\rm ems} \propto N'\Delta_{\rm e}^4|\mu|^2$ where N' is the population on the upper state depending on experimental conditions as well as radiative and nonradiative processes.[30] For a given wavelength range, $\Delta_{\rm e}$ may be looked on as a constant, and therefore $I_{\rm abs}$ ($I_{\rm ems}$) depends mainly on N'' (N') and $|\mu|^2$. For emission intensity, however, the absolute value of $|\mu|^2$ is not significant due to the uncertainty of N', unless two emissions come from a common upper Ω state.

Seven emission bands of OsO have been recorded experimentally by Balfour and Ram,[2] called the 449-nm, 455-nm, 513-nm, 614-nm, 754-nm, 825-nm, and 874-nm systems, respectively, according to the wavelengths (*cf.* Table I in Ref. [2]), but none of them were assigned. In Table 3, we make preliminary assignments for the (0,0) band heads.

In the 449-nm system with $\Delta\Omega = 0$, Balfour and Ram speculated the lower state to be the ground Ω state of OsO,[2] which has a rotational constant of 0.4023 cm^{-1} and a bond length of 1.685 Å. However, in our theoretical results of {1}2, the rotational constant is 0.0136 cm^{-1} larger whereas the bond length is 0.032 Å shorter (see Table 2), exceeding the expected error range of theoretical calculations. Therefore, the lower state should be the other Ω states. In fact, {1}3 and {1}4 are good candidates with consistent rotational constants and bond lengths. With the aid of the quite small rotational constant (B_0) of 0.3657 cm^{-1}, the upper state of the emission band may be easily assigned as {13}3, and the lower state must be {1}3 because of $\Delta\Omega = 0$. However, the transition dipole moment of {13}3 − {1}3 is very small, showing the complexity in the transition mechanism.

Table 3. Assignment of experimental emission bands of $^{192}Os^{16}O$ [a].

Ω state	Method	T_e (cm^{-1})	R_e (Å)	ω_e (cm^{-1})	B_e (cm^{-1})	Note
Lower state (LS)						
{1}2	theory	0	1.653	1027	0.4159	$[1]^3\Pi$ (83)
	Expt.	0				possible LS of the 455-, 614-, 754-, and 874-nm systems
{1}0^+	theory	2035	1.627	992	0.4291	$[1]^1\Sigma^+$ (50) + $[1]^3\Pi$ (38)
	Expt.	E_0				possible LS of the 614- and 874-nm systems.
{1}3	theory	2459	1.676	969	0.4048	$[1]^3\Phi$ (41) + $[1]^5\Delta$ (23) + $[1]^1\Phi$ (15)
	Expt.	E_3		[883] [b]		LS of the 449-, 825-, and probably 513-, 614-, and 874-nm systems
{1}4	theory	3298	1.680	1024	0.4025	$[1]^5\Delta$ (72) + $[1]^3\Phi$ (26)
	Expt.	E_4	1.685	[885]	0.4023	possible LS of the 455- and 614-nm systems
{1}1	theory	3485	1.660	1003	0.4124	$[1]^3\Pi$ (74) +$[1]^5\Delta$ (11)
	Expt.	E_1		[883] [b]		possible LS of the 455-, 513-, 614-, and 754-nm systems
Upper State (US)						
{5}2	theory	11419	1.710	911	0.3970	$[1]^3\Delta$ (49) + $[1]^1\Delta$ (23)
	Expt.	[11432]				possible US of the 874-nm system
{6}1	theory	12676	1.681	1069	0.4028	$[1]^1\Pi$ (47) + $[1]^3\Sigma^-$ (22)
	Expt.	[13253]				possible US of the 754-nm system
{6}0^+	theory	13170	1.670	1199	0.4063	$[1]^3\Pi$ (36) + $[1]^3\Sigma^-$ (17) + $[2]^1\Sigma^+$ (12)
	Expt.	[11432+E_0]				possible US of the 874-nm system
{4}3	theory	13566	1.723	900	0.3805	$[1]^5\Pi$ (56) + $[1]^3\Delta$ (18) + $[2]^3\Delta$ (12)
	Expt.	[13253]				possible US of the 754-nm system
	Expt.	[11432+E_3]				possible US of the 874-nm system
{7}1	theory	13830	1.708	830	0.3941	$[1]^3\Sigma^+$ (21) + $[2]^3\Sigma^-$ (15) + $[2]^3\Pi$ (14)
	Expt.	[13253]				possible US of the 754-nm system
{8}2	theory	14921	1.728	977	0.3850	$[1]^5\Pi$ (65)
	Expt.	[12119+E_3]			[0.3845]	US of the 825-nm system
{9}1	theory	16449	1.719	866	0.3844	$[1]^5\Pi$ (33) + $[1]^3\Delta$ (19) + $[2]^3\Sigma^+$ (10)
	Expt.	[16467]				possible US of the 614-nm system.
{6}3	theory	16531	1.721	920	0.3837	$[2]^3\Delta$ (59) + $[1]^1\Phi$ (16)
	Expt.	[16467]				possible US of the 614-nm system
{9}2	theory	16683	1.714	926	0.3856	$[2]^3\Delta$ (27) + $[1]^3\Delta$ (25) + $[1]^1\Delta$ (23)
	Expt.	[13253+E_1]				possible US of the 754-nm system
{10}1	theory	16844	1.702	1043	0.3874	$[2]^1\Pi$ (30) + $[1]^5\Pi$ (24)+ $[2]^3\Delta$ (17)
	Expt.	[16467]				possible US of the 614-nm system
{7}0^+	theory	16987	1.719	922	0.3838	$[2]^3\Sigma^-$ (43) + $[1]^5\Pi$ (18) + $[2]^1\Sigma^+$ (16)
	Expt.	[13253+E_1]				possible US of the 754-nm system
{12}1	theory	18336	1.703	1007	0.3882	$[2]^3\Delta$ (21) + $[2]^1\Pi$ (17)+ $[1]^3\Delta$ (16)
	Expt.	[16467+E_0]				possible US of the 614-nm system
{4}4	theory	19214	1.706	939	0.3879	$[2]^3\Gamma$ (70) + $[1]^1\Gamma$ (20)
	Expt.	[16467+E_3]				possible US of the 614-nm system
{9}3	theory	19793	1.733	881	0.3782	$[4]^3\Delta$ (26) + $[1]^5\Phi$ (22) + $[1]^7\Sigma^+$ (18)
	Expt.	[16467+E_4]				possible US of the 614 nm system.
{2}5	theory	20230	1.714	898	0.3853	$[2]^3\Gamma$ (84) + $[1]^5\Phi$ (12)
	Expt.	[16467+E_4]				possible US of the 614 nm system.
{9}0^+	theory	20540	1.731	866	0.3817	$[3]^3\Sigma^-$ (38) + $[2]^3\Sigma^-$ (34) + $[3]^1\Sigma^+$ (18)
	Expt.	[16467+E_1]				possible US of the 614-nm system
{10}2	theory	20879	1.748	842	0.3744	$[1]^7\Sigma^+$ (45) + $[2]^5\Pi$ (25) + $[4]^3\Delta$ (12)
	Expt.	[16467+E_1]				possible US of the 614-nm system
{12}2	theory	22412	1.704	923	0.3844	$[3]^3\Delta$ (59) + $[1]^1\Delta$ (17)
	Expt.	[21984]				Possible US of the 455-nm system
{12}3	theory	22746	1.718	939	0.3900	$[4]^3\Delta$ (36) + $[1]^5\Phi$ (29) + $[2]^3\Gamma$ (17)

(Continued on the next page)

	Expt.	[19501+E_3]				possible US of the 513-nm system
{16}1	Theory	22828	1.725	980	0.3851	$[3]^3\Delta$ (28) + $[2]^3\Sigma^+$ (25) + $[2]^3\Sigma^-$ (24)
	Expt.	[19501+E_1]				possible US of the 513-nm system
{6}4	theory	24416	1.710	913	0.3895	$[1]^1\Gamma$ (69) + $[2]^3\Gamma$ (23)
	Expt.	[21984+E_4]				possible US of the 455-nm system
{13}3	theory	24464	1.764	742	0.3682	$[2]^5\Pi$ (54) + $[1]^7\Sigma^+$ (36)
	Expt.	[22277+E_3]		[781]	[0.3657]	US of the 449-nm system
{19}1	theory	24612	1.747	916	0.3813	$[2]^5\Pi$ (49) + $[3]^3\Sigma^-$ (16)
	Expt.	[21984+E_1]				possible US of the 455-nm system

[a] Values in parentheses in the T_e, ω_e, and B_e columns are the experimental T_0, $\Delta G_{1/2}$, and B_0, respectively, from Ref. [2].

[b] Estimated from the 513-nm band system.[2]

The 825-nm system with $\Delta\Omega = \pm 1$ has the same lower state as in the above 449-nm system,[2] i.e. {1}3. According to the experimental excitation energy of 12119 cm^{-1} and the rotational constant (B_0) of 0.3845 cm^{-1}, the upper state may be assigned as {8}2, which comes mainly from $[1]^5\Pi$.

In the 455-, 513-, and 874-nm systems, nothing is known except excitation energies and $\Delta\Omega = 0$. The allowed candidate transitions are {19}1 → {1}1, {12}2 → {1}2, and {6}4 → {1}4 for the 455-nm band system. The other possible transitions are {16}1 → {1}1 and {12}3 → {1}3 for the 513-nm system, and {6}0^+ → {1}0^+, {5}2 → {1}2, and {4}3 → {1}3 for the 874-nm system. The {8}1 → {1}1 transition lies also in the region 874 nm but it is forbidden and therefore may be excluded.

The 614-nm and 754-nm systems are the transitions with $\Delta\Omega = \pm 1$. Due to the lack of experimental rotational constants for comparison, there are more possibilities of allowed candidate transitions. The 614-nm system may be assigned to {12}1 → {1}0^+, {9}0^+/{10}2 → {1}1, {9}1/{10}1/{6}3 → {1}2, {4}4 → {1}3, or {9}3/{2}5 → {1}4, whereas the 754-nm system can be {7}0^+/{9}2 → {1}1 or {6}1/{7}1/{4}3 → {1}2.

4. Conclusion

In this paper, the potential energy curves of low-lying Λ–S states of OsO have been calculated by X2C/MS-NEVPT2, and the fitted spectroscopic constants are compared with the ones by X2C/RMS-CASPT2 and the more accurate X2C/SDSCI+P. The SOC effects are also considered via X2C/MS-NEVPT2/SI to get Ω states. Roos and Malmqvist[19] have shown that the scalar relativistic multi-reference perturbation theory plus SI is applicable to not only *d*-block elements but also actinides, and therefore may be the most feasible scheme for studying the electronic spectra of uranium monoxide.[31]

Theoretical results show that the ground Λ–S and Ω states of OsO are $^1\Sigma^+$ and $^3\Pi_2$, respectively. Based on the theoretical spectroscopic constants and transition dipole moments between Ω states, seven emission bands have been preliminarily assigned. Our results should be useful for guiding future measurements and assignments of near-infrared and visible-ultraviolet spectra of OsO.

Acknowledgements

Project supported by the National Natural Science Foundation of China (Grant No. 22073072) and the Double First-Class University Construction Project of Northwest University.

References

[1] Liu Y, Wang L, Lei Y, Suo B, Zhang Y and Zou W 2023 *Chem. Phys. Lett.* **829** 140692
[2] Balfour W J and Ram R S 1984 *J. Mol. Spectrosc.* **105** 360
[3] Gatterer A, Junkes J, Salpeter E W and Rosen B 1957 *Molecular Spectra of Metallic Oxides* (Vatican City: Specola Vaticana)
[4] Raziunas V, Macur G and Katz S 1965 *J. Chem. Phys.* **43** 1010
[5] Weltner W Jr 1978 *Ber. Bunsenges. Phys. Chem.* **82** 80
[6] Zhou M, Citra A, Liang B and Andrews L 2000 *J. Phys. Chem. A* **104** 3457
[7] Yao C, Guan W, Song P, Su Z M, Feng J D, Yan L K and Wu Z J 2007 *Theor. Chem. Acc.* **117** 115
[8] Dai G L and Wang C F 2012 *Russ. J. Phys. Chem. A* **86** 798
[9] Liu W and Peng D 2009 *J. Chem. Phys.* **131** 031104
[10] Peng D and Reiher M 2012 *Theor. Chem. Acc.* **131** 1081
[11] Zobel J P, Widmark P O and Veryazov V 2020 *J. Chem. Theory Comput.* **16** 278
[12] Zobel J P, Widmark P O and Veryazov V 2021 *J. Chem. Theory Comput.* **17** 3233
[13] Battaglia S and Lindh R 2021 *J. Chem. Phys.* **154** 034102
[14] Angeli C, Borini S, Cestari M and Cimiraglia R 2004 *J. Chem. Phys.* **121** 4043
[15] Forsberg N and Malmqvist P Å 1997 *Chem. Phys. Lett.* **274** 196
[16] Ghigo G, Roos B O and Malmqvist P Å 2004 *Chem. Phys. Lett.* **396** 142
[17] Malmqvist P Å and Roos B O 1989 *Chem. Phys. Lett.* **155** 189
[18] Schimmelpfennig B 1996 *AMFI: atomic mean field integral program* (Stockholm: University of Stockholm, Sweden)
[19] Roos B O and Malmqvist P Å 2004 *Phys. Chem. Chem. Phys.* **6** 2919
[20] Zhang Y, Suo B, Wang Z, Zhang N, Li Z, Lei Y, Zou W, Gao J, Peng D, Pu Z, Xiao Y, Sun Q, Wang F, Ma Y, Wang X, Guo Y and Liu W 2020 *J. Chem. Phys.* **152** 064113
[21] Suo B, Lei Y, Han H and Wang Y 2018 *Mol. Phys.* **116** 1051
[22] Fdez Galván I, Vacher M, Alavi A, *et al.* 2019 *J. Chem. Theory Comput.* **15** 5925
[23] Aquilante F, Autschbach J, Baiardi A, *et al.* 2020 *J. Chem. Phys.* **152** 214117

[24] Le Roy R J 2017 *J. Quantum Spectrosc. Radiat. Transfer* **186** 167
[25] Liu W and Hoffmann M R 2014 *Theor. Chem. Acc.* **133** 1481
[26] Song Y, Guo Y, Lei Y, Zhang N and Liu W 2021 *Top. Curr. Chem.* **379** 43
[27] Glendening E D, Badenhoop J K, Reed A E, Carpenter J E, Bohmann J A, Morales C M, Landis C R and Weinhold F 2013 *NBO version* 6.0 (Theoretical Chemistry Institute, University of Wisconsin, Madison, WI)
[28] Kraka E, Larsson J A and Cremer D 2010 *Computational Spectroscopy*, ed. Grunenberg J (New York: Wiley) pp. 105–149
[29] Kalescky R, Kraka E and Cremer D 2013 *J. Phys. Chem. A* **117** 8981
[30] Herzberg G 1950 *Molecular Spectra and Molecular Structure*, Vol. I, *Spectra of Diatomic Molecules*, 2nd Edn. (Princeton: D. Van Nostrand) pp. 18–21
[31] Bai X L, Zhang X D, Zhang F Q and Steimle T C 2022 *Chin. Phys. B* **31** 053301